



# Understanding the regio- and chemoselective polar [3+2] cycloaddition of the Padwa carbonyl ylides with $\alpha$ -methylene ketones. A DFT study

Wafaa Benchouk<sup>a</sup>, Sidi Mohamed Mekelleche<sup>a,\*</sup>, Maria José Aurell<sup>b</sup>, Luis Ramón Domingo<sup>b,\*</sup>

<sup>a</sup>Département de Chimie, Faculté des Sciences, Université A. Belkaid, B. P. 119, Tlemcen, 13000, Algeria

<sup>b</sup>Departamento de Química Orgánica, Universidad de Valencia, Dr. Moliner 50, 46100 Burjassot, Valencia, Spain

## ARTICLE INFO

### Article history:

Received 5 March 2009

Received in revised form 8 April 2009

Accepted 9 April 2009

Available online 17 April 2009

### Keywords:

Polar [3+2] cycloadditions

Padwa carbonyl ylides

Electron localization function

Electrophilicity

Nucleophilicity

Density functional theory

## ABSTRACT

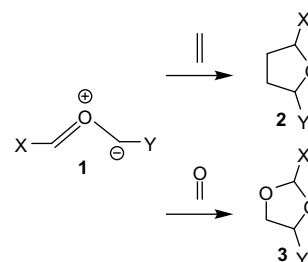
The regio- and chemoselective polar [3+2] cycloaddition (32CA) of the Padwa carbonyl ylide (CY) with  $\alpha$ -methylene ketone ( $\alpha$ MK) to yield the oxo-bridged spirocycloadduct has been studied using the DFT method at the B3LYP/6-31G(d) computational level. Six reactive channels associated to the stereo-, regio-, and chemoselective approach modes of the CY to the C=C and C=O reactive sites of the  $\alpha$ MK have been analyzed. DFT calculations for this cycloaddition are in complete agreement with the experimental outcome, explaining the reactivity and selectivity of the formation of the [3+2] cycloadduct. Analysis of the global and local electrophilicity and nucleophilicity indices allows an explanation about the regio- and chemoselectivity of this 32CA reaction. Intrinsic reaction coordinate (IRC) calculations and the topological analysis of the electron localization function (ELF) of the relevant points of the favored reactive channel explain the one-step *two-stage* nature of the mechanism of this cycloaddition.

© 2009 Elsevier Ltd. All rights reserved.

## 1. Introduction

Cycloaddition reactions are one of the most important processes with both synthetic and mechanistic interest in organic chemistry. Current understanding of the underlying principles in the [3+2] cycloadditions (32CA) has grown from a fruitful interplay between theory and experiment.<sup>1</sup> The general concept of 1,3-dipolar cycloadditions was introduced by Huisgen and co-workers in the early 1960s.<sup>2</sup> Huisgen's work stated the basis for the understanding of the mechanism of concerted cycloaddition reactions. In the last decades, in addition of the reaction mechanism, the understanding of the selectivity behaviors of the 32CA reactions continues to present a real challenge. We note that the chemo-, regio-, and stereoselectivity of these reactions may be controlled either by choosing the appropriate substrates or by controlling the reaction using a Lewis acid or a metal complex acting as catalyst.

32CA reactions of carbonyl ylide (CY) **1** with  $\pi$ -bonds of olefins or carbonyl groups present an attractive strategy for the construction of tetrahydrofuran **2** or dioxolane **3** systems (see Scheme 1).<sup>3</sup> CYs are very reactive species that quickly react when they are formed with unsaturated systems. As a consequence, the cycloaddition reaction of CY systems constitutes the last step of a domino reaction, which is



Scheme 1.

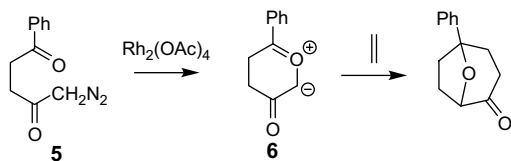
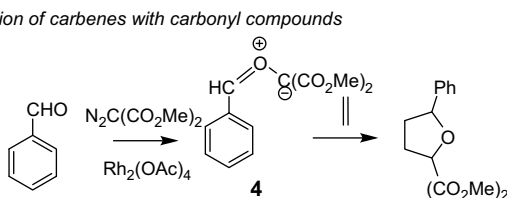
\* Corresponding authors. Fax: +34 96 354 3106.

E-mail address: [domingo@utopia.uv.es](mailto:domingo@utopia.uv.es) (L.R. Domingo).

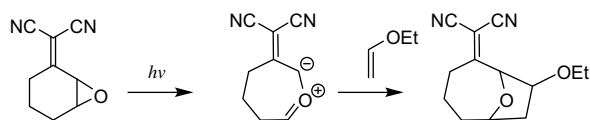
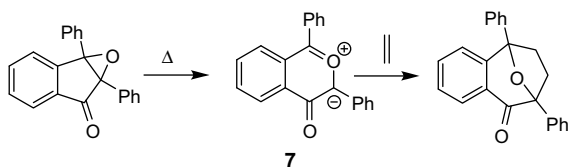
initialized by the formation of these reactive intermediates. There are mainly two methods to generate CYs (see Scheme 2): (i) reaction of a carbene generated in situ by the rhodium catalyzed decomposition of a diazo compound with a carbonyl compound<sup>4</sup> and (ii) the thermal<sup>5</sup> or photoinduced<sup>6</sup> ring-aperture of epoxides.

The 32CA reactions of the CYs have been theoretically studied using both semiempirical<sup>6,7</sup> and density functional theory (DFT)<sup>8,9</sup> methods. These studies reveal that the analysis of the different reaction channels of these cycloadditions explains correctly the stereo-, regio-, and chemoselectivities experimentally observed. Recently, Molchanov et al.<sup>9</sup> studied the 32CA reaction of a series of 3-substituted cyclopropenes **8** with the CY **9** to yield the formally [3+2] cycloadducts **10** (see Scheme 3). A frontier molecular orbital

## a) reaction of carbenes with carbonyl compounds



## b) thermal and photoinduced ring-aperture of epoxides

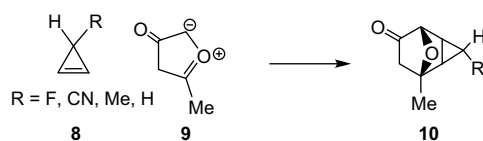


Formation of carbonyl ylides

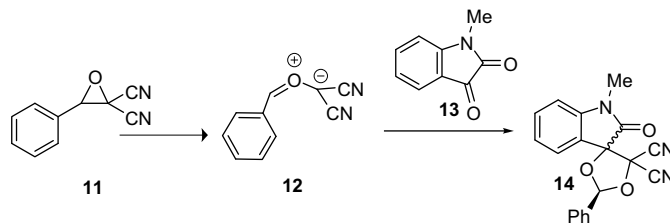
Scheme 2.

(FMO) study, based on the prediction of  $\text{HOMO}_{\text{cyclopropene}}\text{-LUMO}_{\text{CY}}$  interactions, has been also performed by these authors.<sup>9</sup> However, it turns out that the FMO analysis fails to predict the order of reactivity of cyclopropenes **8**, which might be taken as the difference between the corresponding dominant  $\Delta E_{\text{(L-H)}}$  values for different cyclopropenes. In return, the analysis of the electrophilicity,  $\omega$ ,<sup>10</sup> of CY **9** and the cyclopropenes **8** pointed out the electrophilic character of the CY **9** and the nucleophilic character of **8**. The difference in global electrophilicity,  $\Delta\omega$ ,<sup>11</sup> of both reagents was in quantitative agreement with the experimental order of reactivity of the cyclopropenes. B3LYP/6-311++G(d,p) calculations performed for the preferential *exo* approach of the cyclopropene **8** (R=H) to the CY **9** showed that the cycloaddition has a very low activation barrier of about 2 kcal mol<sup>-1</sup>.<sup>9</sup> The distances of the two forming bonds at the transition state structure (TS), 2.74 and 2.86 Å, indicated a slightly asynchronous concerted mechanism of this polar cycloaddition. The activation free energies associated to the cycloaddition increased with the electron-withdrawing substitution on cyclopropenes in clear agreement with the experimental outcomes.<sup>9</sup>

Very recently, Mongin and Domingo have experimentally and theoretically reported the 32CA reaction of isatin **13** with the electrophilically activated CY **12** generated by the thermal ring-aperture of the epoxide **11** (see Scheme 4).<sup>12</sup> This reaction presented a low stereoselectivity but a complete regio- and chemoselectivity to yield the spirocycloadducts **14**. The more favorable reactive channels were associated to the nucleophilic attack of the carbonyl oxygen



Scheme 3.



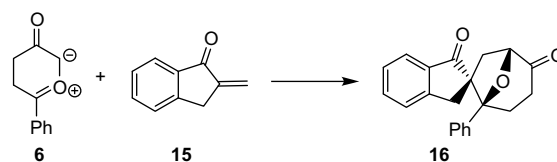
Scheme 4.

atom of isatin **13** to the more electrophilic center of the CY **12**, the phenyl substituted carbon atom. Analysis of the electrophilicity<sup>10</sup> of the reagents showed that the larger electrophilic character of the CY **12**,  $\omega=4.29$  eV, than the isatin **13**,  $\omega=2.71$  eV, is responsible for the nucleophilic behavior of the later.<sup>12</sup> This behavior, which is in complete agreement with the energy and geometry analysis of the TSs, allows to explain the regio- and chemoselectivity experimentally observed in these 32CA reactions. A further experimental and theoretical study of the 32CA reactions of the CY **12** with aldehydes and imines established the high electrophilic character of the CY **12** and its participation in polar 32CA reactions.<sup>13</sup>

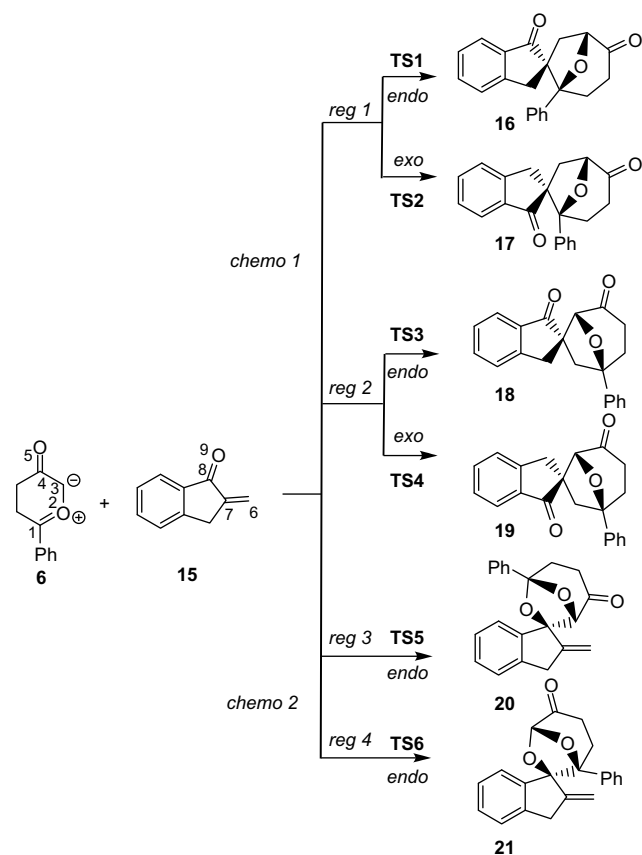
Our aim in the present study is to present a theoretical study of the 32CA reaction of the Padwa CY **6**, which is usually obtained by decomposition of diazo compound **5** in presence of rhodium acetate catalyst<sup>14</sup> (see Scheme 2). In this context, Muthusamy et al.<sup>15</sup> have recently reported the stereo-, regio-, and chemoselective synthesis of oxa-bridged spirocycles by the 32CA reaction of the Padwa CY **6** with the  $\alpha$ -methylene ketone ( $\alpha$ MK) **15** (see Scheme 5). Consequently, we have selected this reaction as a computational model for the cycloaddition reactions of the Padwa CYs. A comparative analysis of this 32CA reaction with those recently reported by us<sup>12,13</sup> will allow to give a deeper insight on the mechanism of the 32CA reaction involving CYs and an advanced understanding of the regio- and the chemoselectivity experimentally observed.

## 2. Computational methods

All calculations were carried out with the Gaussian03 suite of programs.<sup>16</sup> DFT calculations were carried out using the B3LYP<sup>17</sup> exchange-correlation functionals, together with the standard 6-31G(d) basis set.<sup>18</sup> The optimizations were carried out using the Bery analytical gradient optimization method.<sup>19</sup> The stationary points were characterized by frequency calculations in order to verify that TSs had one and only one imaginary frequency. The intrinsic reaction coordinate (IRC)<sup>20</sup> path was traced in order to check the energy profiles connecting each TS to the two associated minima of the proposed mechanism using the second order González-Schlegel integration method.<sup>21</sup> The values of enthalpies, entropies, and free energies were calculated with the standard statistical thermodynamics at 298.15 K.<sup>18</sup> The frequency data used for thermochemical analysis were scaled by a factor of 0.96. The electronic structures of stationary points were analyzed by the natural bond orbital (NBO) method<sup>22</sup> and the topological analysis of the electron localization function (ELF),  $\eta(r)$ .<sup>23</sup> The ELF study was performed with the TopMod program.<sup>24</sup>



Scheme 5.



Scheme 6.

Solvent effects have been considered at the same level of theory by geometry optimization of the gas-phase structures using a self-consistent reaction field (SCRf)<sup>25</sup> based on the polarizable continuum model (PCM) of the Tomasi's group.<sup>26</sup> Since this cycloaddition is carried out in dichloromethane (DCM), we have selected its dielectric constant at 298.0 K,  $\epsilon=8.93$ .

The global electrophilicity index,<sup>10</sup>  $\omega$ , which measures the stabilization energy when the system acquires an additional electronic charge  $\Delta N$  from the environment, has been given by the following simple expression,<sup>10</sup>  $\omega=(\mu^2/2\eta)$ , in terms of the electronic chemical potential  $\mu$  and the chemical hardness  $\eta$ . Both quantities may be approached in terms of the one electron energies of the frontier molecular orbital HOMO and LUMO,  $\epsilon_H$  and  $\epsilon_L$ , as  $\mu \approx (\epsilon_H + \epsilon_L)/2$  and  $\eta \approx (\epsilon_L - \epsilon_H)$ , respectively.<sup>27</sup> Recently, we have introduced an empirical (relative) nucleophilicity index,<sup>28</sup>  $N$ , based on the HOMO energies obtained within the Kohn–Sham scheme,<sup>29</sup> and defined as  $N = E_{\text{HOMO}}(\text{Nu}) - E_{\text{HOMO}}(\text{TCE})$ . This nucleophilicity scale is referred to tetracyanoethylene (TCE) taken as a reference. The reactivity indices were computed from the B3LYP/6-31G(d) HOMO and LUMO energies at the ground state of the molecules. Local electrophilicity<sup>30</sup> and nucleophilicity<sup>31</sup> indices,  $\omega_k$  and  $N_k$ , were evaluated using the following expressions:  $\omega_k = \omega f_k^+$  and  $N_k = N f_k^-$  where  $f_k^+$  and  $f_k^-$  are the Fukui functions for a nucleophilic and electrophilic attacks, respectively.<sup>32</sup>

### 3. Results and discussions

#### 3.1. Mechanistic study of the 32CA reaction of the Padwa carbonyl ylide **6** with the $\alpha$ -methylene ketone **15**

Due to the existence of two C=C and C=O reactive sites on the  $\alpha$ MK **15**, and the asymmetry of both reagents, this cycloaddition

reaction can yield up to eight isomeric oxa-bridged spirocycloadducts. The formation of these cycloadducts can be related to the chemo-, regio-, and stereoselectivity of this 32CA reaction. The experimental results indicate that this cycloaddition reaction is characterized by a complete chemoselectivity, with the unique participation of the C=C double bond, and with a complete regioselectivity, with the unique formation of the regioisomer associated with the formation of the C3–C6 and C1–C7  $\sigma$  bonds (see Scheme 6). The experimental results also indicate that the *endo* approach is remarkably more favored in comparison with the *exo* approach, indicating a large stereoselectivity of this 32CA reaction. In order to explain the chemo-, regio-, and stereoselectivity experimentally observed, six reactive channels were elaborated and analyzed (see Scheme 6). These reactive channels are related the *endo* and *exo* approaches associated with the two regioisomeric attack modes, *reg1* and *reg2*, of the CY **6** to the C=C double bond of the  $\alpha$ MK **15**, *chemo1*, and the *endo* channels associated with the two regioisomeric attack modes, *reg3* and *reg4*, of the CY **6** to the C=O double bond of the  $\alpha$ MK **15**, *chemo2*. The analysis of the stationary points, involved in the potential energy surface of this 32CA, indicates that this cycloaddition follows a one-step mechanism. Hence, six TSs, **TS1**, **TS2**, **TS3**, **TS4**, **TS5**, and **TS6**, and the corresponding oxa-bridged spirocycloadducts **16–21** were located and characterized (see Scheme 6). The energy results are summarized in Table 1.

The most favorable reactive channels correspond to the formation of the *endo* and *exo* stereoisomeric oxa-bridged spirocycloadducts **16** and **17**, via **TS1** and **TS2**, respectively (*reg1*). The TSs are located 1.8 (**TS1**) and 2.8 kcal mol<sup>-1</sup> (**TS2**) above the reagents. These very low reaction barriers are closer to those obtained for the 32CA reactions of the CY **9** with cyclopropene **8**, 1.6 kcal mol<sup>-1</sup>,<sup>9</sup> and of the CY **12** with benzaldehyde, 2.6 kcal mol<sup>-1</sup>.<sup>13</sup> The low energy difference between **TS1** and **TS2**,  $\Delta\Delta E^\ddagger=1.0$  kcal mol<sup>-1</sup>, points to a low stereoselectivity.<sup>13</sup> Note that in gas phase, the major stereoisomer **16** has the *endo* stereochemistry. The *endo* and *exo* regioisomeric **TS3** and **TS4** are located 4.2 and 3.7 kcal mol<sup>-1</sup> above **TS1** (*reg2*). These large energy differences prevent the formation of the regioisomeric cycloadducts **18** and **19**, a fact that is in clear agreement with experimental results. We note the inversion of the stereoselectivity for the regioisomeric channel *reg2*. Indeed, the *exo* **TS4** is located 0.5 kcal mol<sup>-1</sup> below the *endo* **TS3**. Finally, the two *endo* regioisomeric channels associated with the attacks to the C=O double bond are 5.1 (**TS5**) and 11.9 (**TS6**) kcal mol<sup>-1</sup> more energetic than **TS1** associated with the *endo* attack of the C=C double bond. These large energy differences

Table 1

Total ( $E$ , in au) and relative<sup>a</sup> ( $\Delta E$ , in kcal mol<sup>-1</sup>) energies in gas phase and in DCM for the 32CA reaction of the carbonyl ylide **6** and the  $\alpha$ -methylene ketone **15**

	Gas phase		Dichloromethane	
	$E$	$\Delta E$	$E$	$\Delta E$
<b>6</b>	-575.569906		-575.584838	
<b>15</b>	-461.093759		-461.102788	
<b>TS1</b>	-1036.660835	1.8	-1036.679333	5.2
<b>TS2</b>	-1036.659218	2.8	-1036.678456	5.8
<b>TS3</b>	-1036.654159	6.0	-1036.672795	9.3
<b>TS4</b>	-1036.654961	5.5	-1036.673919	8.6
<b>TS5</b>	-1036.652642	6.9	-1036.669140	11.6
<b>TS6</b>	-1036.641765	13.7	-1036.656763	19.3
<b>16</b>	-1036.742037	-49.2	-1036.757239	-43.7
<b>17</b>	-1036.736839	-45.9	-1036.754531	-42.0
<b>18</b>	-1036.742104	-49.2	-1036.758555	-44.5
<b>19</b>	-1036.741189	-48.6	-1036.757128	-43.6
<b>20</b>	-1036.711330	-29.9	-1036.724547	-23.2
<b>21</b>	-1036.699938	-22.8	-1036.713637	-16.3

<sup>a</sup> Relative to reactants (**6+15**).

**Table 2**Thermodynamic data, in DCM and at 25 °C, for the 32CA reaction of the carbonyl ylide **6** and the  $\alpha$ -methylene ketone **15**

	<i>H</i> au	$\Delta H^{\ddagger}$ kcal mol <sup>-1</sup>	<i>S</i> cal mol <sup>-1</sup> K <sup>-1</sup>	$\Delta S^{\ddagger}$ cal mol <sup>-1</sup> K <sup>-1</sup>	<i>G</i> au	$\Delta G^{\ddagger}$ kcal mol <sup>-1</sup>
<b>6</b>	-575.397608		103.1		-575.446569	
<b>15</b>	-460.949159		91.2		-460.992471	
<b>TS1</b>	-1036.336682	6.3	149.0	-45.2	-1036.407495	19.8
<b>TS2</b>	-1036.336036	6.7	151.4	-42.8	-1036.407968	19.5
<b>TS3</b>	-1036.330140	10.4	147.8	-46.4	-1036.400362	24.3
<b>TS4</b>	-1036.331334	9.7	149.2	-45.1	-1036.402200	23.1
<b>TS5</b>	-1036.326944	12.4	147.1	-47.1	-1036.396830	26.5
<b>TS6</b>	-1036.315091	19.9	145.7	-48.5	-1036.384333	34.3
<b>16</b>	-1036.411564	-40.7	135.6	-58.6	-1036.475992	-23.2
<b>17</b>	-1036.408002	-38.4	142.9	-51.4	-1036.475872	-23.1
<b>18</b>	-1036.412058	-41.0	144.7	-49.5	-1036.480825	-26.2
<b>19</b>	-1036.410637	-40.1	145.7	-48.5	-1036.479878	-25.6
<b>20</b>	-1036.379763	-20.7	145.1	-49.1	-1036.448688	-6.1
<b>21</b>	-1036.368437	-13.6	141.8	-52.4	-1036.435798	2.0

<sup>a</sup> Relative to reactants (**6**+**15**).

prevent the formation of the chemoisomeric cycloadducts **20** and **21**. Finally, all 32CA channels are strongly exothermic: between -49.2 and -45.9 kcal mol<sup>-1</sup> for the participation of the C=C double bond, and between -29.9 and -22.8 kcal mol<sup>-1</sup> for the participation of the C=O double one.

Solvent effects on cycloaddition reactions are well known, and they have received considerable attention. The solvent effects have been examined by B3LYP/6-31G(d) optimizations of stationary points using a relatively simple SCRf method, based on the PCM of Tomasi's group.<sup>26</sup> The energy results are summarized in Table 1. With the inclusion of solvent effects, the reactants are more stabilized than TSs and cycloadducts. As a consequence, in DCM, the activation barriers associated with **TS1** and **TS2** increase to 5.2 and 5.8 kcal mol<sup>-1</sup>, respectively. In DCM, the stereo-, regio-, and chemoselectivity of the 32CA reaction between **6** and **15** decrease slightly,  $\Delta\Delta E^{\ddagger}$  (**TS1**-**TS2**)=0.6,  $\Delta\Delta E^{\ddagger}$  (**TS1**-**TS4**)=3.4, and  $\Delta\Delta E^{\ddagger}$  (**TS1**-**TS5**)=6.4 kcal mol<sup>-1</sup>.

Finally, the relative free energies in DCM for the six reactive channels were computed. The energy results are summarized in Table 2. After the inclusion of the zero-point energy and thermal corrections to the electronic energies and entropies, the activation free energies of **TS1** and **TS2** rise to 19.8 and 19.5 kcal mol<sup>-1</sup>. These high values are a consequence of the unfavorable activation entropies associated with this bimolecular process. Note that there is a slight change of the stereoselectivity as a consequence of the larger activation entropy associates to the *endo* **TS1**, -45.2 cal mol<sup>-1</sup> K<sup>-1</sup>, than that to the *exo* **TS2**, -42.8 cal mol<sup>-1</sup> K<sup>-1</sup>. Therefore, the calculations carried out in gas phase and in DCM show clearly that this 32CA reaction is characterized by a low stereoselectivity.<sup>13</sup> The more favorable *exo* regioisomeric **TS4**, remains 3.6 kcal mol<sup>-1</sup> above **TS2**, while the more favorable chemoselective channel via **TS5** remains 7.0 kcal mol<sup>-1</sup> above **TS2**. The reaction channels associated with the participation of the C=C double bond of the  $\alpha$ MK **15**, *chemo1*, are strongly exergonic; between -23 and -26 kcal mol<sup>-1</sup>. Consequently, this 32CA reaction can be considered irreversible.

The geometries of the TSs associated with the six reactive channels are displayed in Figure 1. A comparative analysis of the TSs obtained in gas phase and in DCM indicates that the inclusion of solvent effects on the geometry optimization produces minor changes relative to the gas-phase geometries. At the TSs associated with the participation of the C=C double bond of the  $\alpha$ MK **15**, *chemo1*, the lengths of the forming bonds are 2.353 Å (C3-C6) and 2.899 Å (C1-C7) at **TS1** and 2.252 Å (C3-C6) and 3.187 Å (C1-C7) at **TS2**, while at the regioisomeric TSs are 2.335 Å (C1-C6) and 2.601 Å (C3-C7) at **TS3**, 2.382 Å (C1-C6) and 2.606 Å (C3-C7) at **TS4**. At the TSs associated with the participation of the C=O double bond of the  $\alpha$ MK **15**, *chemo2*, the lengths of the forming bonds at the two

regioisomeric TSs are 2.108 Å (C1-O9) and 2.253 Å (C3-C8) at **TS5**, 2.656 Å (C1-C8) and 1.872 Å (C3-O9) at **TS6**.

The extent of the asynchronicity of the bond formation in a cycloaddition reaction can be measured through the difference between the lengths of the two  $\sigma$  bonds that are being formed in the reaction, i.e.,  $\Delta r = \text{dist1} - \text{dist2}$ . For the four reactive channels associated with the participation of the C=C double bond of the  $\alpha$ MK **15**, *chemo1*, the asynchronicity at the TSs is 0.55 at **TS1**, 0.94 at **TS2**, 0.27 at **TS3**, and 0.22 at **TS4**. Two conclusions can be redraw from these values: (i) the TSs associated to the more favorable regioisomeric paths *reg1* are more asynchronous than those associated with the regioisomeric path *reg2*; and (ii) at these asynchronous TSs, the shorter distance corresponds to the C-C bond formation at the  $\beta$ -conjugated position of the  $\alpha$ MK **15**.

The extent of bond formation along a reaction pathway is provided by the concept of bond order (BO).<sup>33</sup> At the TSs associated with the participation of the C=C double bond of the  $\alpha$ MK **15**, the BO values of the two forming bonds are: 0.22 (C3-C6) and 0.08 (C1-C7) at **TS1**, 0.31 (C3-C6) and 0.09 (C1-C7) at **TS2**, 0.29 (C1-C6) and 0.19 (C3-C7) at **TS3**, 0.27 (C1-C6) and 0.16 (C3-C7) at **TS4**, while at the TSs associated with the participation of the C=O double bond the BO values of the two forming bonds are: 0.27 (C1-O9) and 0.33 (C3-C8) at **TS5**, 0.20 (C1-C8) and 0.42 (C3-O9) at **TS6**. The less energetic *endo* **TS1** is earlier than the *exo* **TS2**. At these stereoisomeric TSs, the low BO values associated to the C1-C7 forming bond indicate that this bond is not being formed at the TS. The BO values at the regioisomeric **TS3** and **TS4** point out asynchronous concerted bond formation processes. The BO values at the four TSs associated with the attacks to the C=C double bond of  $\alpha$ MK **15** point out that this species controls the asynchronicity on the bond formation. Note that the formation of the C3-C6 bond, which involves the  $\beta$ -conjugated position of  $\alpha$ MK **15**, is more advanced than the formation of the C1-C7 one. This behavior allows to assert the observation that in an asynchronous bond formation associated with a polar cycloaddition process the  $\sigma$  bond formation at the more electrophilic center of the electrophile is formed in a larger extension.<sup>34</sup> Finally, the BO values of the two forming bonds at the two unfavorable chemoselective channels point to also asynchronous concerted bond formation processes.

The IRC from **TS1** to the cycloadduct **16** indicates that this cycloaddition has a two-stage mechanism;<sup>35</sup> that is, while at the first stage of the reaction only the C3-C6 bond is being formed, the second stage is associated to the C1-C7 bond formation. We would like to point out that at the **HP** structure, located at the half of the IRC curve, the C3-C6 bond formation is very advanced, 1.610 Å, whereas the C1-C7 bond is very delayed, 2.499 Å (see Fig. 2).<sup>36</sup> At **HP**, the BO values of the C3-C6 and C1-C7 forming bonds are 0.91 and 0.40, respectively.

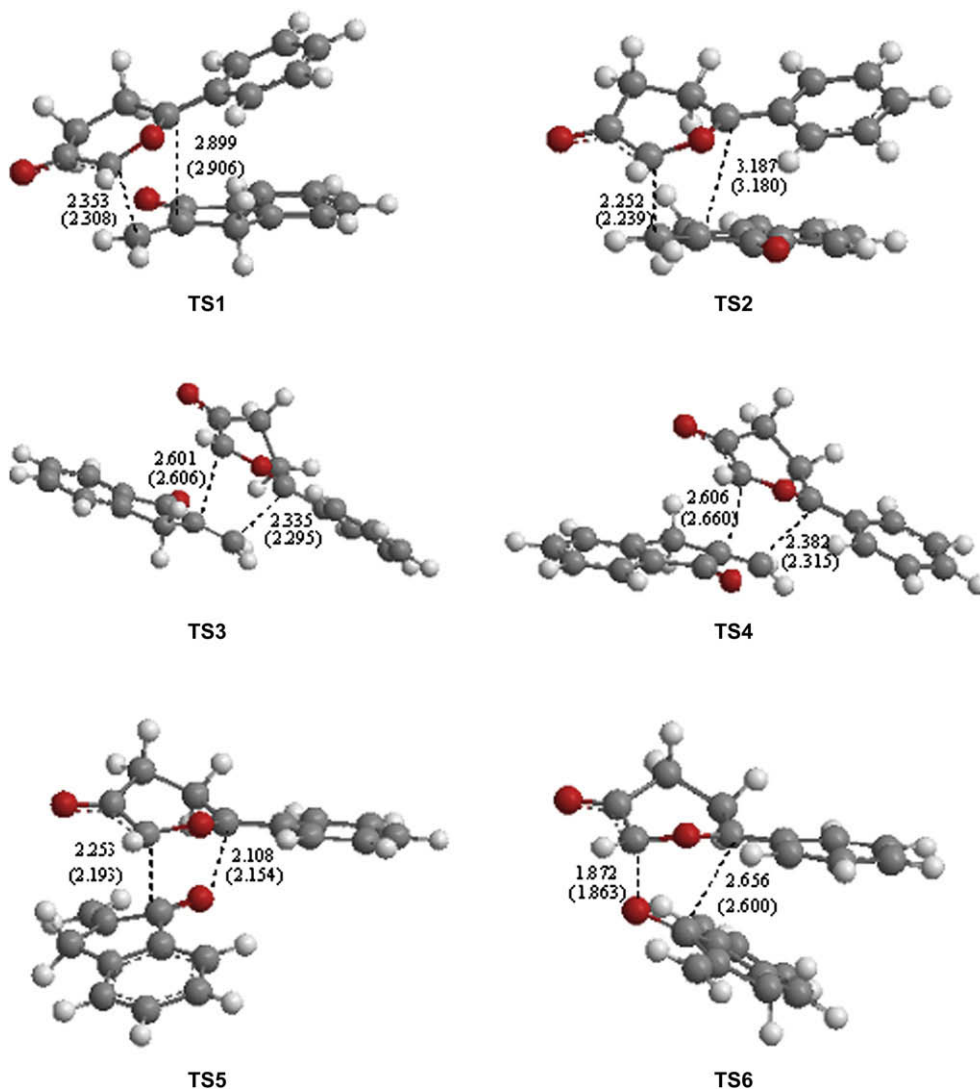


**Figure 1.** Transition structures for the 32CA reaction of the carbonyl ylide **6** and the  $\alpha$ -methylene ketone **15**; the values of the bond lengths directly involved in the processes are given in Å; the values in parentheses correspond to the reaction in DCM.

The natural population analysis (NPA) allows us to evaluate the charge transfer (CT) at the TSs. The natural charges at the TSs were shared between the CY **6** and the  $\alpha$ MK **15** fragments. The CT from **6** to **15** at the TSs are: 0.15e at **TS1**, 0.17e at **TS2**, 0.09e at **TS3**, 0.09e at **TS4**, 0.24e at **TS5**, and 0.25e at **TS6**. At the TSs associated with the attack of the C=C double bond, *chemo1*, the CT at the more favorable regioisomeric **TS1** and **TS2** is larger than that at **TS3** and **TS4**. The more unfavorable **TS6** presents the larger CT of this series of TSs. This behavior is a consequence of the more advance character of the TS. At the **HP** structure, the CT from CY **6** to  $\alpha$ MK **15** is 0.26e. Along the nucleophilic attack of the CY **6** to the  $\alpha$ MK **15**, there is an increase of the CT to reach the point **HP**. Along the second stage of the reaction, there is a decrease of the CT as a consequence of a back-donation until the formation of the electronically balances [3+2] cycloadduct **16**.<sup>13</sup> For instance, the CT for the structure located at the halfway between **HP** and cycloadduct **16** is decreased to 0.16e.

### 3.2. Topological analysis of the ELF

The topology of the ELF of the Padwa CY **6**, the  $\alpha$ MK **15**, the **TS1**, the **HP** structure, and the oxa-bridged spirocycloadduct **16** was

analyzed in order to obtain additional information about the electron density evolution in this 32CA reaction.<sup>36,37</sup> Our aim is to give a deeper insight to the electronic nature and the charge rearrangement along this polar cycloaddition process.<sup>13</sup>

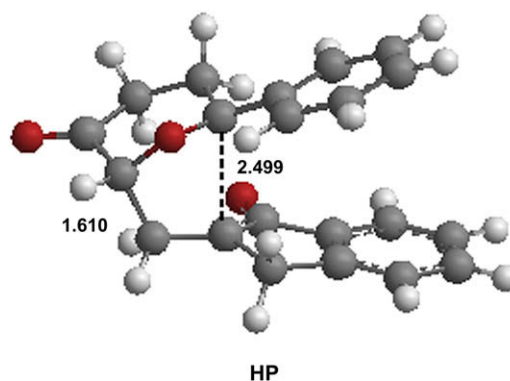


**Figure 2.** **HP** structure located at the half of IRC from **TS1** to **16** for the 32CA reaction of the carbonyl ylide **6** and the  $\alpha$ -methylene ketone **15**; the values of the bond lengths directly involved in the processes are given in Å.

**Table 3**

The valence basin population  $N$  calculated for the ELF of the reagents, the **TS1**, **HP**, and the cycloadduct **16** involved in the more favorable *endo* pathway of the 32CA reaction of the carbonyl ylide **6** and the  $\alpha$ -methylene ketone **15**

Basin	Basin population $N [e]$				
	<b>6</b> and <b>15</b>	<b>TS1</b>	<b>HP</b>	<b>16</b>	
<b>6</b>	V(C1,O2)	2.02	1.90	1.49	1.28
	V(O2,C3)	1.81	1.72	1.32	1.23
	V(C3,C4)	2.91	2.51	2.14	2.13
	V(C4,O5)	2.17	2.28	2.38	2.39
	V(O5)	2.71	2.71	2.62	2.58
	V'(O5)	2.74	2.73	2.65	2.63
	V(C1)	—	—	0.52	—
	V(O2)	3.55	3.84	4.65	2.60
	V'(O2)	—	—	—	2.46
	V(C3)	0.57	0.72	—	—
	V(C1,C7)	—	—	—	1.94
	V(C3,C6)	—	—	1.82	1.88
	<b>15</b>	V(C7)	—	—	0.55
V(C6,C7)		1.82	3.35	2.11	1.88
V'(C6,C7)		1.69	—	—	—
V(C7,C8)		2.22	2.42	2.58	2.11
V(C8,O9)		2.34	2.24	2.31	2.31
V(O9)		2.66	2.64	2.71	2.63
V'(O9)		2.62	2.79	2.81	2.66

The Becke and Edgecombe's ELF<sup>38</sup> is derived from the measure of the Fermi hole curvature and interpreted in terms of local excess kinetic energy due to Pauli repulsion. It is confined to the [1,0] interval in order to tend to 1 where parallel spins are highly improbable, and where therefore there is a high probability of opposite spin pairs, and to zero in regions where there is a high probability of same spin pairs. The topological partition of the ELF gradient field<sup>39</sup> yields basins of attractors, which can be thought as corresponding to the bonds and lone pairs of the Lewis's picture. In a molecule, two types of basins are found: the core basins surrounding nuclei of atomic number  $Z > 2$  and labeled C(A), where A is the atomic symbol of the element, and on the valence basins. The valence basins are characterized by the number of atomic valence shells to which they belong called the synaptic order. A monosynaptic basin V(A) corresponds to a lone pair on atom A, a disynaptic basin V(A,B) to a two-center bond linking A and B, a trisynaptic basin V(A,B,C) to a three center bond and so on. A population analysis can be further carried out by integrating the charge density over the basin volumes whereas the calculation of the covariance matrix of the basin population enables to quantify delocalization.<sup>40</sup>

The populations  $N$  of the more relevant valence basins of these structures are listed in Table 3. A schematic representation of the electron population evolution along the cycloaddition is given in Scheme 7. Padwa CY **6** presents eight valence basins, namely V(C1,O2), V(O2,C3), V(C3,C4), V(C4,O5), V(O2), two V(O5) and V(C3). The more significant valence basins of the CY **6** are the V(O2) monosynaptic basin on the O2 oxygen atom,  $N=3.55e$ , and the V(C3) monosynaptic basin on the C3 carbon atom,  $N=0.57e$ . The V(C3) basin points out some nucleophilic character of this CY. The more relevant valence basins of the  $\alpha$ MK **15** are the two V(C6,C7) basins, with a total population of  $3.51e$ , associated with the C6=C7 double bond, the V(C7,C8) basin,  $N=2.22e$ , and the V(C8–O9) basin,  $N=2.34e$ , associated with the C8=O9 double bond.

The unique relevant change found at the ELF of **TS1** relative to the reagents is the fusion of the two disynaptic basins V(C6,C7) in **15** into one disynaptic basin V(C6,C7) with a population of  $3.35e$ . A slight increase in the electron population of the monosynaptic basins on the O2 oxygen atom and the C3 carbon atom is observed. We note that **TS1** has not monosynaptic basins on the C1, C6, and C7 carbon atoms, which will be created in a subsequent step, and prior to the formation of the corresponding  $\sigma$  bonds.<sup>37b</sup> The amount of

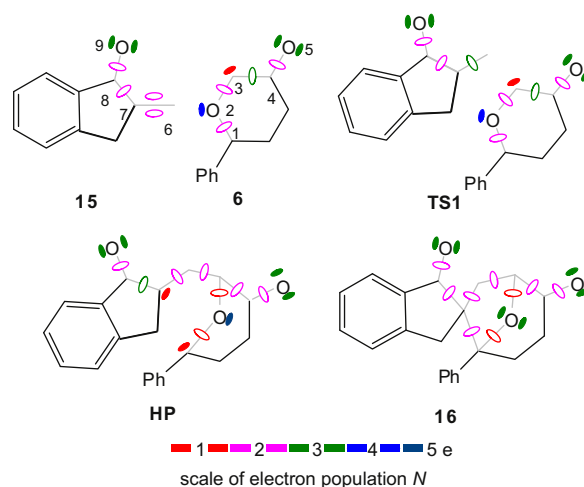
the CT in this polar process has been evaluated from the sum of the core and valence basins of the Padwa CY **6** fragment in **TS1**. The population analysis based on the topological region shows that the carbonyl ylide fragment is positively charged ( $+0.17e$ ) in **TS1**. This value is closer to that obtained from the NBO analysis.<sup>36,37b</sup>

The most interesting changes in the electron population along the IRC are observed for the **HP** structure for which the creation of the disynaptic basin V(C3,C6), with a population of  $1.82e$ , points out the complete C3–C6 bond formation. It is important to note that at the **HP** structure, two new monosynaptic basins are created on the C1 and C7 atoms with an electron population of  $0.52e$  and  $0.55e$ , respectively. These two monosynaptic basins will be responsible to the C1–C7 bond formation, which takes place at the last part of the IRC (see Scheme 7). Finally, for the cycloadduct **16**, the ELF analysis shows the presence of two disynaptic basins V(C1,C7) and V(C3,C6) with an electron population of  $1.94e$  and  $1.88e$ , respectively. These basins correspond, obviously, to the two new  $\sigma$  bonds C1–C7 and C3–C6. The population analysis based on the topological regions indicates that at **HP** the positive charge at the carbonyl ylide fragment increases to  $0.38e$ . This result is in complete agreement with the NBO analysis made at **HP** and discussed above.<sup>36</sup> This large CT found along the C3–C6 bond formation, indicates the polar nature of this highly asynchronous 32CA reaction, which is anticipated by the electrophilicity/nucleophilicity analysis of reagents (see later).

### 3.3. Analysis based on the global and local reactivity indexes at the ground state of the reagents

Recent studies carried out on cycloaddition reactions have shown that the analysis of the reactivity indices defined within the conceptual DFT<sup>41</sup> is a powerful tool to study the reactivity in polar cycloadditions.<sup>11,30,34</sup> In Table 4, the static global properties (electronic chemical potential,  $\mu$ , chemical hardness,  $\eta$ , global electrophilicity,  $\omega$ , and global nucleophilicity,  $N$ ) of the CYs **6** and **12** and  $\alpha$ -methylene ketones **15**, **22**, **23**, and **24** are presented.

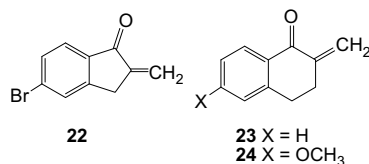
The electronic chemical potential of the Padwa CY **6**,  $-0.1378$  au, is higher than the electronic chemical potential of  $\alpha$ MK **15**,  $-0.1557$  au, thereby indicating that along a polar cycloaddition, the net CT will take place from the CY **6** to the  $\alpha$ MK **15**. Note that the electronic chemical potential of the CY **12**,  $-0.1693$  au, is lower than that of benzaldehyde,  $-0.1590$  au, and *N*-methyl-benzylimine,  $-0.1379$  au, thereby indicating that in these cases the CT flux toward the CY **12**.<sup>13</sup>



**Scheme 7.** Schematic representation of the more relevant monosynaptic,  $\bullet$ , and disynaptic,  $\circ$ , valence basins.

**Table 4**

Electronic chemical potential,  $\mu$ , and chemical hardness,  $\eta$ , in au, global electrophilicity,  $\omega$ , and global nucleophilicity,  $N$ , in eV, for the carbonyl ylides **6** and **12** and the  $\alpha$ -methylene ketones **15** and **22–24**



	$\mu$	$\eta$	$\omega$	$N$
<b>12</b>	-0.1693	0.0908	4.29	3.28
<b>6</b>	-0.1378	0.0915	2.82	4.50
<b>22</b>	-0.1639	0.1713	2.13	2.33
<b>15</b>	-0.1557	0.1723	1.91	2.91
<b>23</b>	-0.1547	0.1762	1.85	2.51
<b>24</b>	-0.1423	0.1678	1.64	2.97

The electrophilicity of the Padwa CY **6**,  $\omega=2.82$  eV, allows to classify this species as a strong electrophile within the electrophilicity scale.<sup>11</sup> This value is lower than that found at the CY **12**,  $\omega=4.29$  eV.<sup>13</sup> On the other hand, the CY **6** presents a large nucleophilicity value,  $N=4.50$  eV, a value that is higher than that found at the CY **12**,  $N=3.28$  eV. Therefore, an opposite behavior is found between the Padwa CY **6** and the Mongin CY **12**. That is, while the CY **12** will behave as a strong electrophile, the Padwa CY **6** will behave as a good nucleophile.

The  $\alpha$ MK **15** has an electrophilicity value of  $\omega=1.91$  eV, being classified also a strong electrophile.<sup>11</sup> The inclusion of an electron-withdrawing bromine atom on the aryl ring of **15** increases remarkably the electrophilicity of the  $\alpha$ MK **22**,  $\omega=2.13$  eV. The  $\alpha$ MK **15** has also a large nucleophilicity value,  $N=2.91$  eV, which decreases to 2.33 eV at the bromine derivative **22**. On the other hand, the decrease of the ring strain from a five-membered in **15** to a six-membered one in **23** involves a slight decrease of both electrophilicity and nucleophilicity indexes.<sup>42</sup> Finally, the inclusion of an electron-releasing methoxy group on the aryl ring of  $\alpha$ MK **23** decreases the electrophilicity of the  $\alpha$ MK **24**,  $\omega=1.64$  eV, and increases the nucleophilicity,  $N=2.97$  eV (see Table 4). The decrease of the electrophilicity of the corresponding  $\alpha$ MKs, **22**>**15**>**24**, is in reasonable agreement with the decrease of the reactivity of these  $\alpha$ MKs.<sup>15</sup>

The best descriptors for studying local reactivity and regioselectivity for a polar reaction will be the local electrophilicity<sup>30</sup> and the local nucleophilicity.<sup>31</sup> In a polar cycloaddition reaction between unsymmetrical reagents, the more favorable two-center interaction will take place between the more electrophile center, characterized by the highest value of the local electrophilicity index  $\omega_k$  at the electrophile, and the more nucleophile center, characterized by the highest value of the local nucleophilicity index  $N_k$  at the nucleophile.<sup>30</sup> In Table 5 the local electrophilicity,  $\omega_k$ , and nucleophilicity,  $N_k$ , indices of the CY **6** and the  $\alpha$ MK **15** are presented. For the CY **6**, the more electrophilic center corresponds with the phenyl substituted C1 carbon,  $\omega_1=0.68$  eV, while the more nucleophilic center corresponds with the C3 carbon,  $N_3=1.82$  eV. For the  $\alpha$ MK **15**, the more electrophilic center corresponds to the

**Table 5**

Local electrophilicity,  $\omega_k$ , and local nucleophilicity,  $N_k$ , values (in eV) of the carbonyl ylide **6**, and the  $\alpha$ -methylene ketone **15**

	$\omega_k$				$N_k$			
	C1	C3			C1	C3		
<b>6</b>	0.68	0.37			0.80	1.82		
<b>15</b>	C6	C7	C8	O9	C6	C7	C8	O9
	0.43	0.11	0.37	0.33	0.24	0.34	0.13	1.91

methylene carbon,  $\omega_6=0.43$  eV, while the more nucleophilic center corresponds to the O9 oxygen,  $N_9=1.91$  eV. As a consequence, the more favorable polar interaction will take place between the more nucleophilic center of the CY **6**, the C3 carbon, and the more electrophilic center of  $\alpha$ MK **15**, the C6 carbon. This analysis is in clear agreement with the geometrical and electronic structures of **TS1** and **TS2**, which show that the C3–C6 bond formation is more advanced than the C1–C7 bond formation. If we consider the sum of the  $\omega_k+N_k$  values at the two feasible interactions that take place along the **6**+**15** reaction, 2.25 eV ( $\omega_6+N_3$ ) along the C3/C6 two-center interaction and 1.02 eV ( $N_7+\omega_1$ ) along the C1/C7 two-center interaction, we can see that the former is clearly favored. These results are in total agreement with the regio- and the chemoselectivity experimentally observed.<sup>15</sup>

The analysis of the reactivity indices indicates that both reagents involved in the 32CA reactions of the CY **12** with aldehydes and imines have electrophilic and nucleophilic behaviors.<sup>13</sup> However, the NBO and ELF analyses, performed for the more favorable regioisomeric TS involved in the cycloaddition reaction with imines, indicate that at the highly asynchronous processes the bond formation is more advanced at the more electrophilic carbon atom of the CY **12** and that the CY residue is being negatively charged, in clear agreement with the large electrophilic character of the CY **12**.<sup>13</sup> However, in the cycloaddition reaction involving the Padwa CY **6**, the bond formation is more advanced at the more nucleophilic carbon atom of this CY, and the CY residue is being positively charged. Thus, our analysis points out that the CYs can participate in polar cycloadditions as good electrophiles or as good nucleophiles. These behaviors, which can be anticipated by the analysis of the static reactivity indices, allow to explain the very low activation barriers found in these 32CA reactions.

#### 4. Conclusions

The stereo-, regio-, and chemoselective 32CA of the Padwa CY **6** with  $\alpha$ MK **15** to yield the oxo-bridged spirocycloadduct **16** have been studied using DFT methods at the B3LYP/6-31G(d) computational level. This 32CA presents a one-step mechanism with a polar character. Six reactive channels associated to the stereo-, regio-, and chemoselective approach modes of the CY **6** to the C=C and C=O reactive sites of the  $\alpha$ MK **15** have been analyzed. The more favorable *endo* and *exo* stereoisomeric reactive channels, which have *two-stage* mechanisms, are associated with the nucleophilic attack of the C3 atom of the CY **6** to the  $\beta$ -conjugated position of  $\alpha$ MK **15**. DFT calculations, performed both in gas phase and in DCM, yield energies and free energies for the transition state structures in clear agreement with experimental regio- and chemoselectivity.

The present study allows to distinguish the unlike electrophilic/nucleophilic behaviors of the Padwa CY **6** in comparison with the one recently obtained by Mongin by thermal ring-aperture of an epoxide, the CY **12**. While the CY **6** behaves as a good nucleophile, the CY **12** behaves as a strong electrophile. This finding allows to explain the regioselectivity of these CYs toward C=C and C=O  $\pi$  systems. IRC calculations combined to the topological ELF analysis explain suitably the one-step *two-stage* mechanism of this cycloaddition. Finally, the analysis of the global electrophilicity and nucleophilicity indices allows an explanation about the participation of the CYs as either good electrophiles or good nucleophiles in polar cycloadditions. For this polar process, the analysis of the local electrophilicity and nucleophilicity indices allows the rationalization of the regio- and the chemoselectivity experimentally observed.

#### Acknowledgements

This work was supported by research funds provided by the Ministerio de Ciencia e Innovación of the Spanish Government

(project CTQ2006-14297/BQU). We thank Professor Bernard Silvi for helpful comments.

## References and notes

- (a) Padwa, A. *1,3-Dipolar Cycloaddition Chemistry*; Wiley-Interscience: New York, NY, 1984; Vols. 1–2; (b) Padwa, A. *Comprehensive Organic Chemistry*; Pergamon: Oxford, 1991; Vol. 4, pp 1069–1109.
- (a) Huisgen, R. *Angew. Chem., Int. Ed. Engl.* **1963**, *2*, 565; (b) Huisgen, R. *Angew. Chem., Int. Ed. Engl.* **1967**, *6*, 16.
- (a) Mehta, G.; Muthusamy, S. *Tetrahedron* **2002**, *58*, 9477; (b) Padwa, A.; Weingarten, M. D. *Chem. Rev.* **1996**, *96*, 223; (c) Hodgson, D. M.; Pierard, F. Y. T. M.; Stuppel, P. A. *Chem. Soc. Rev.* **2001**, *30*, 50.
- (a) Padwa, A.; Hornbuckle, S. F.; Fryxell, G. E.; Stull, P. D. *J. Org. Chem.* **1989**, *54*, 817; (b) Nair, V.; Mathai, S.; Nair, S. M.; Rath, N. P. *Tetrahedron Lett.* **2003**, *44*, 8407; (c) Nair, V.; Mathai, S.; Mathew, S. C.; Rath, N. P. *Tetrahedron* **2005**, *61*, 2849.
- (a) Ruf, S. G.; Dietz, J.; Regitz, M. *Tetrahedron* **2000**, *56*, 6259; (b) Wang, G.-W.; Yang, H.-T.; Wu, P.; Miao, C.-B.; Xu, Y. J. *Org. Chem.* **2006**, *71*, 4346; (c) Bentabed, G.; Rahmouni, M.; Mongin, F.; Derdour, A.; Hamelin, J.; Bazureau, J. P. *Synth. Commun.* **2007**, *37*, 2935.
- Kotera, M.; Ishii, K.; Tamura, O.; Sakamoto, M. *J. Chem. Soc., Perkin Trans. 1* **1998**, 313.
- Muthusamy, S.; Babu, S. A.; Gunanathan, C.; Ganguly, B.; Suresh, E.; Dastidar, P. *J. Org. Chem.* **2002**, *67*, 8019.
- (a) Celik, M. A.; Yurtsever, M.; Tuzun, N. S.; Gungor, F. S.; Sezer, O.; Anac, O. *Organometallics* **2007**, *26*, 2978; (b) Suga, H.; Ebiura, Y.; Fukushima, K.; Kakehi, A.; Baba, T. *J. Org. Chem.* **2005**, *70*, 10782.
- Diev, V. V.; Kostikov, R. R.; Gleiter, R.; Molchanov, A. P. *J. Org. Chem.* **2006**, *71*, 4066.
- Parr, R. G.; von Szentpaly, L.; Liu, S. *J. Am. Chem. Soc.* **1999**, *121*, 1922.
- (a) Domingo, L. R.; Aurell, M. J.; Perez, P.; Contreras, R. *Tetrahedron* **2002**, *58*, 4417; (b) Perez, P.; Domingo, L. R.; Aurell, M. J.; Contreras, R. *Tetrahedron* **2003**, *59*, 3117; (c) Pérez, P.; Domingo, L. R.; Aizman, A.; Contreras, R. The Electrophilicity Index in Organic Chemistry. In *Theoretical Aspects of Chemical Reactivity*; Toro-Labbé, A., Ed.; Elsevier Science: Oxford, 2007; Vol. 19, p 139.
- Bentabed-Ababsa, G.; Derdour, A.; Roisnel, T.; Sáez, J. A.; Domingo, L. R.; Mongin, F. *Org. Biomol. Chem.* **2008**, *6*, 3144.
- Bentabed-Ababsa, G.; Derdour, A.; Roisnel, T.; Sáez, J. A.; Pérez, P.; Chamorro, E.; Domingo, L. R.; Mongin, F. *J. Org. Chem.* **2009**, *74*, 2120.
- Padwa, A.; Hornbuckle, S. F. *Chem. Rev.* **1991**, *91*, 263.
- Muthusamy, S.; Krishnamurthi, J.; Munirathnam Nethaji, M. *Chem. Commun.* **2005**, 3862.
- Frisch, M. J.; Trucks, G. W.; Schlegel, H. B.; Scuseria, G. E.; Robb, M. A.; Cheeseman, J. R.; Montgomery, J. J. A.; Vreven, T.; Kudin, K. N.; Burant, J. C.; Millam, J. M.; Iyengar, S. S.; Tomasi, J.; Barone, V.; Mennucci, B.; Cossi, M.; Scalmani, G.; Rega, N.; Petersson, G. A.; Nakatsuji, H.; Hada, M.; Ehara, M.; Toyota, K.; Fukuda, R.; Hasegawa, J.; Ishida, M.; Nakajima, T.; Honda, Y.; Kitao, O.; Nakai, H.; Klene, M.; Li, X.; Knox, J. E.; Hratchian, H. P.; Cross, J. B.; Adamo, C.; Jaramillo, J.; Gomperts, R.; Stratmann, R. E.; Yazyev, O.; Austin, A. J.; Cammi, R.; Pomelli, C.; Ochterski, J. W.; Ayala, P. Y.; Morokuma, K.; Voth, G. A.; Salvador, P.; Dannenberg, J. J.; Zakrzewski, V. G.; Dapprich, S.; Daniels, A. D.; Strain, M. C.; Farkas, O.; Malick, D. K.; Rabuck, A. D.; Raghavachari, K.; Foresman, J. B.; Ortiz, J. V.; Cui, Q.; Baboul, A. G.; Clifford, S.; Cioslowski, J.; Stefanov, B. B.; Liu, G.; Liashenko, A.; Piskorz, P.; Komaromi, I.; Martin, R. L.; Fox, D. J.; Keith, T.; Al-Laham, M. A.; Peng, C. Y.; Nanayakkara, A.; Challacombe, M.; Gill, P. M. W.; Johnson, B.; Chen, W.; Wong, M. W.; Gonzalez, C.; Pople, J. A. *Gaussian03*; Gaussian: Wallingford CT, 2004.
- (a) Becke, A. D. *J. Chem. Phys.* **1993**, *98*, 5648; (b) Lee, C.; Yang, W.; Parr, R. G. *Phys. Rev. B* **1988**, *37*, 785.
- Hehre, W. J.; Radom, L.; Schleyer, P. v. R.; Pople, J. A. *Ab Initio Molecular Orbital Theory*; Wiley: New York, NY, 1986.
- (a) Schlegel, H. B. *J. Comput. Chem.* **1982**, *3*, 214; (b) Schlegel, H. B. Geometry Optimization on Potential Energy Surface. In *Modern Electronic Structure Theory*, Yarkony D. R., Ed.; World Scientific Publishing: Singapore, 1994.
- Fukui, K. *J. Phys. Chem.* **1970**, *74*, 4161.
- (a) González, C.; Schlegel, H. B. *J. Phys. Chem.* **1990**, *94*, 5523; (b) González, C.; Schlegel, H. B. *J. Chem. Phys.* **1991**, *95*, 5853.
- (a) Reed, A. E.; Curtiss, L. A.; Weinhold, F. *Chem. Rev.* **1988**, *88*, 899; (b) Reed, A. E.; Weinstock, R. B.; Weinhold, F. *J. Chem. Phys.* **1985**, *83*, 735.
- (a) Savin, A.; Becke, A. D.; Flad, J.; Nesper, R.; Preuss, H.; Vonscherner, H. G. *Angew. Chem., Int. Ed. Engl.* **1991**, *30*, 409; (b) Savin, A.; Silvi, B.; Colonna, F. *Can. J. Chem.* **1996**, *74*, 1088; (c) Savin, A.; Nesper, R.; Wengert, S.; Fassler, T. F. *Angew. Chem., Int. Ed.* **1997**, *36*, 1809; (d) Silvi, B. *J. Mol. Struct.* **2002**, *614*, 3.
- Noury, S.; Krokidis, X.; Fuster, F.; Silvi, B. *Comput. Chem.* **1999**, *23*, 597.
- (a) Tomasi, J.; Persico, M. *Chem. Rev.* **1994**, *94*, 2027; (b) Simkin, B. Y.; Sheikhet, I. *Quantum Chemical and Statistical Theory of Solutions-A Computational Approach*; Ellis Horwood: London, 1995.
- (a) Cancès, E.; Mennucci, B.; Tomasi, J. *J. Chem. Phys.* **1997**, *107*, 3032; (b) Cossi, M.; Barone, V.; Cammi, R.; Tomasi, J. *Chem. Phys. Lett.* **1996**, *255*, 327; (c) Barone, V.; Cossi, M.; Tomasi, J. *J. Comput. Chem.* **1998**, *19*, 404.
- (a) Parr, R. G.; Pearson, R. G. *J. Am. Chem. Soc.* **1983**, *105*, 7512; (b) Parr, R. G.; Yang, W. *Density Functional Theory of Atoms and Molecules*; Oxford University Press: New York, NY, 1989.
- Domingo, L. R.; Chamorro, E.; Pérez, P. *J. Org. Chem.* **2008**, *73*, 4615.
- Kohn, W.; Sham, L. J. *Phys. Rev.* **1965**, *140*, 1133.
- Domingo, L. R.; Aurell, M. J.; Perez, P.; Contreras, R. *J. Phys. Chem. A* **2002**, *106*, 6871.
- (a) Contreras, R.; Andres, J.; Safont, V. S.; Campodonico, P.; Santos, J. G. *J. Phys. Chem. A* **2003**, *107*, 5588; (b) Pérez, P.; Domingo, L. R.; Duque-Noreña, M.; Chamorro, E. *J. Mol. Struct. (Theochem)* **2009**, *895*, 86.
- Parr, R. G.; Yang, W. *J. Am. Chem. Soc.* **1984**, *106*, 4049.
- Wiberg, K. B. *Tetrahedron* **1968**, *24*, 1083.
- Aurell, M. J.; Domingo, L. R.; Perez, P.; Contreras, R. *Tetrahedron* **2004**, *60*, 11503.
- (a) Goldstein, M. J.; Thayer, G. L., Jr. *J. Am. Chem. Soc.* **1965**, *87*, 1933; (b) Domingo, L. R.; Saéz, J. A.; Zaragoza, R. J.; Arnó, M. J. *Org. Chem.* **2008**, *73*, 8791.
- Domingo, L. R.; Picher, M. T.; Arroyo, P.; Saez, J. A. *J. Org. Chem.* **2006**, *71*, 9319.
- (a) Berski, S.; Andres, J.; Silvi, B.; Domingo, L. R. *J. Phys. Chem. A* **2003**, *107*, 6014; (b) Domingo, L. R.; Picher, M. T.; Arroyo, P. *Eur. J. Org. Chem.* **2006**, 2570; (c) Berski, S.; Andres, J.; Silvi, B.; Domingo, L. R. *J. Phys. Chem. A* **2006**, *110*, 13939; (d) Polo, V.; Andres, J.; Berski, S.; Domingo, L. R.; Silvi, B. *J. Phys. Chem. A* **2008**, *112*, 7128.
- (a) Becke, A. D.; Edgecombe, K. E. *J. Chem. Phys.* **1990**, *92*, 5397; (b) Dobson, J. F. *J. Chem. Phys.* **1991**, *94*, 4328; (c) Savin, A.; Jepsen, O.; Flad, J.; Andersen, O. K.; Preuss, H.; von Schnering, H. G. *Angew. Chem., Int. Ed. Engl.* **1992**, *31*, 187; (d) Silvi, B. *J. Phys. Chem. A* **2003**, *107*, 3081.
- (a) Silvi, B.; Savin, A. *Nature* **1994**, *371*, 683; (b) Häussermann, U.; Wengert, S.; Nesper, R. *Angew. Chem., Int. Ed. Engl.* **1994**, *33*, 2069.
- (a) Silvi, B. *Phys. Chem. Phys.* **2004**, *6*, 256; (b) Poater, J.; Duran, M.; Solà, M.; Silvi, B. *Chem. Rev.* **2005**, *105*, 3911.
- (a) Geerlings, P.; De Proft, F.; Langenaeker, W. *Chem. Rev.* **2003**, *103*, 1793; (b) Ess, D. H.; Jones, G. O.; Houk, K. N. *Adv. Synth. Catal.* **2006**, *348*, 2337.
- Domingo, L. R.; Perez, P.; Contreras, R. *Eur. J. Org. Chem.* **2006**, 498.